ELSEVIER

Physica B 318 (2002) 267–271

PHYSICA B

www.elsevier.com/locate/physb

# Spin-polarized electron momentum density distributions $REMn_2Ge_2$ (RE = Gd, La)

J.W. Taylor[a,*], J.A. Duffy[a], A.M. Bebb[a], M.J. Cooper[a], M.R. Lees[a], S. Majumdar[a], J.E. McCarthy[b], D.N. Timms[c], C. Detlefs[b], P.C. Canfield[d]

[a] *Department of Physics, The University of Warwick, Coventry, CV4 7AL, UK*
[b] *European Synchrotron Radiation Facility, BP 220, F-38043, Grenoble Cedex, France*
[c] *School of Earth and Environmental science, The University of Portsmouth, Portsmouth, PO1 2DT, UK*
[d] *Ames Laboratory, 59 Physics, Iowa State University, Ames, IA 50011, USA*

**Abstract**

The spin-polarized electron momentum distributions (EMD) for ferrimagnetic $GdMn_2Ge_2$ and ferromagnetic $LaMn_2Ge_2$ have been measured using the magnetic Compton scattering technique. The spin-polarized EMDs were resolved along the *c*-axis at 15 K. In the Gd sample, the Gd and Mn spin sublattices are aligned antiparallel with spin moments of $6.8\pm0.1\mu_B$ per formula unit ($FU^{-1}$) and $3.7\pm0.1\mu_B$ $FU^{-1}$, respectively, with the Gd spin sublattice oriented parallel to the scattering vector. The ferromagnetic La system exhibits no 4f moment and the Mn moment is aligned parallel to the scattering vector, the ordered spin moment on the Mn being $2.4\pm0.1\mu_B$ $FU^{-1}$. The two samples measured are the extreme points of the phase diagram for $Gd_{1-x}La_xMn_2Ge_2$. Our data give a direct indication of the sublattice reorientation at $x\approx0.5$, implied from previous magnetization measurements and indicate that at a low temperature the Mn sublattice is a canted ferromagnetic system. 

*PACS:* 75.25.+z; 75.30.Kz; 75.50.Gg

*Keywords:* Magnetic compton; Spin polarized electron momentum density

## 1. Introduction

The magnetic phase diagram of the naturally layered intermetallic compound $Gd_{1-x}La_xMn_2Ge_2$, exhibits a wide variety of magnetic phenomena [1,2] as a function of temperature and La doping. Reentrant ferromagnetism, meta-magnetism, and two distinct regions of ferrimagnetism have been observed along with regions of collinear and non-collinear ferromagnetism. In this paper we present the spin-polarized electron momentum distribution of $GdMn_2Ge_2$ and $LaMn_2Ge_2$, the compounds at the extremes of the doping phase diagram. The results demonstrate that the Mn–Mn spin sublattice undergoes a reorientation as the system is doped with Gd.

Previous studies of this system have concentrated on bulk magnetization measurements [3], from which the separated Mn–Mn and Gd sublattice magnetization can only be inferred, by applying models of varied complexity, such as the interlayer coupling model [4], and the

*Corresponding author.
*E-mail address:* jonathan.taylor@warwick.ac.uk (J.W. Taylor).

0921-4526/02/$ - see front matter 
PII: S0921-4526(02)00786-X

two-sublattice ferromagnetic molecular field model [3]. Intermetallic compounds, of the form $REMn_2Ge_2$, where RE is a rare-earth, crystallize in the $ThCr_2Si_2$ tetragonal structure with space group I4/mmm in the naturally layered sequence Mn–Ge–RE–Ge–Mn, along the $c$-axis [5,6] in such a way as to form two planes of Mn atoms. The inter and intralayer Mn–Mn distance in these compounds is known to be a critical factor in determining the magnetic ordering temperatures, and the temperature dependence of the bulk magnetization. Changes in the lattice parameter either from thermal effects or from magnetostriction, critically alter the Mn–Mn intra and interlayer spacing and hence exchange energies, thus giving rise to the complex magnetism/meta-magnetism associated with these compounds. Recent work [17] has implied that the RE exchange potential is weak in comparison to that from the Mn sublattice. The parent compound $GdMn_2Ge_2$ is antiferromagnetic below $\approx 350$ K. The system undergoes a ferromagnetic phase quasi-first-order phase transition at 93 K to a ferrimagnetic structure. In the low-temperature ferrimagnetic phase $T < 93$ K, the Mn sublattices consist of a canted arrangement of Mn spins ferromagnetically coupled in the planes and ferromagnetically coupled between the Mn–Mn planes, while the RE sublattice is coupled antiferromagnetically. The degree of canting of the Mn spin sublattice is a complex function of temperature [7]. At a low temperature, the ordered Gd sublattice stabilizes the system to produce a two-sublattice ferrimagnet, with a non-collinear arrangement of spins on the Mn sublattice.

Single crystal samples of $LaMn_2Ge_2$ and $GdMn_2Ge_2$ were flux grown, using starting materials of at least 4N purity, in the form of thin platelets with the surface of the plate normal to the $c$-axis of the system. The structure and quality of the samples were confirm using Laue photography.

## 2. Magnetic compton scattering

The Compton effect is observed when high-energy photons are inelastically scattered by electrons. The scattered photon energy distribution is Doppler-broadened, since the electrons have a finite momentum distribution. If the scattering event is described within the impulse approximation [8] then the measured Compton spectrum is directly proportional to the scattering cross-section [9].

The Compton profile is defined as a 1D projection onto the scattering vector of the electron momentum distribution, $n(\mathbf{p})$, where the scattering vector is taken parallel to the $z$-direction

$$J(p_z) = \int\int n(\mathbf{p})\,\mathrm{d}p_x\,\mathrm{d}p_y. \tag{1}$$

The integral of $J(p_z)$ is the total number of electrons per unit cell.

Magnetic Compton scattering (MCS) is a probe uniquely sensitive to the spin component of a material's magnetization. If the incident beam has a component of circular polarization, the scattering cross-section contains a term which is spin dependent [10]. In order to isolate the spin dependence one must either flip the sample's direction of magnetization parallel and antiparallel with respect to the scattering vector or change the 'handedness' of the photon helicity. Either method results in a magnetic Compton profile (MCP), $J_{\mathrm{mag}}(p_z)$, that is dependent upon only the unpaired spin in the sample, and is defined as the 1D projection of the spin polarized electron momentum density

$$J_{\mathrm{mag}}(p_z) = \int\int [n^{\uparrow}(\mathbf{p}) - n^{\downarrow}(\mathbf{p})]\,\mathrm{d}p_x\,\mathrm{d}p_y. \tag{2}$$

Here, $n^{\uparrow}(\mathbf{p})$ and $n^{\downarrow}(\mathbf{p})$ are the momentum densities of the majority and minority spin bands. The integral of the MCP is the total spin moment $\mathrm{FU}^{-1}$ in the sample. MCS is an established technique for determining spin polarized electron densities [11–13]. Within the impulse approximation, the method is insensitive to the orbital moment [14]. Unlike MXCD, MCS samples all the spin polarized electrons regardless of their binding energies and wavefunction symmetries.

## 3. Experiment and data analysis

The magnetic Compton profiles of $LaMn_2Ge_2$ and $GdMn_2Ge_2$ were resolved along the $c$-axis as a

function of temperature at the high-energy beamline ID15A at the ESRF. The experiment was performed in reflection geometry at a temperature of 15 K. The temperature-controlled sample environment constituted of a closed cycle He refrigerator. An incident beam energy of 220 keV was selected using an Si 311 monochromator in Laué geometry. At these photon energies, which are desirable for optimum resolution and interpretation within the impulse approximation, reversing the helicity of the incident photons is not yet practical. The spin-dependent signal was isolated by reversing the sample's magnetization vector using a 1 T electromagnet. Circular polarization was produced by selecting a beam approximately 2 μrad below the orbital plane of the synchrotron [15], this value was chosen to maximize the ratio of magnetic scattering to statistical noise in the charge scattering. A degree of circular polarization of about 45% was obtained. The energy spectrum of the scattered flux was measured using a 13 element Ge detector at a mean scattering angle of 170°. The momentum resolution of the magnetic Compton spectrometer, taken as the FWHM of the instrument response function, was 0.40 a.u. (where $1\ \text{a.u.} = 1.99 \times 10^{-24}\ \text{kg m s}^{-1}$).

The total number of counts in the charge Compton profiles was $2 \times 10^8$ corresponding to a statistical precision of $\pm 2\%$ in the resulting MCP, in a bin width of 0.1 a.u. Since the MCP is the difference between two charge Compton profiles, components arising from spin-paired electrons and from most sources of systematic error are effectively cancelled out. The data were corrected for energy-dependent detector efficiency, sample absorption, and the relativistic scattering cross-section. The magnitude of the magnetic multiple scattering was determined to be no more than 0.012%. The profiles were corrected for multiple scattering using the technique described by Felstiener [16]. After checking that the resulting spectra were symmetric about $p_z = 0$, the profiles were folded to improve the effective statistics. The profile areas were normalized to an absolute spin moment scale using Fe data taken under the same conditions.

## 4. Results and discussion

### 4.1. Spin polarized EMD in $LaMn_2Ge_2$ and $GdMn_2Ge_2$

The experimental spin-polarized EMD for $LaMn_2Ge_2$, resolved along the $c$-axis at 15 K is shown in Fig. 1.

The measured spin moment was determined to be $2.5 \pm 0.1 \mu_B\ FU^{-1}$ corresponding to $1.25 \mu_B$ per Mn site. The value is in good agreement with that taken previously using bulk measurements and implies that the Mn–Mn sublattice has a non-collinear structure. In this phase, the Mn sublattice is seen to align parallel to the scattering vector. MCP is shown compared with a relativistic Hartree Fock (RHF) free atom profile for 3d Mn, demonstrating that the measured signal is 3d in nature. The dip observed in the experimental data results from the solid state effect on the d band spin-polarized electrons, which are not accounted for in the RHF calculation.

Fig. 2 shows the experimentally measured EMD for $GdMn_2Ge_2$ resolved along the $c$-axis at 15 K.

The measured profile is significantly different, the 4f moment is now parallel to the scattering vector, with the Mn sublattice aligned antiparallel to it. Localized features in real space equate to broad delocalized features in momentum space,

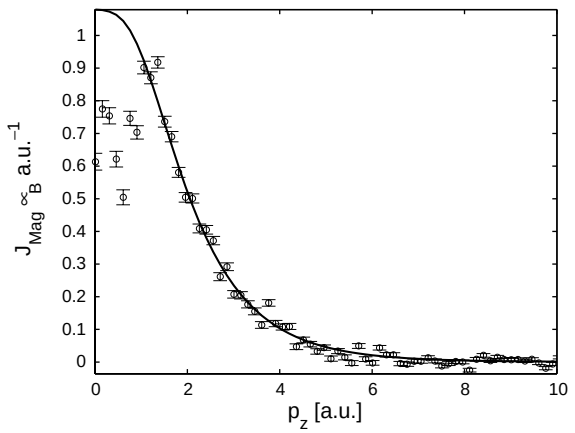


Fig. 1. The experimental magnetic Compton profile (MCP) (circle) of $LaMn_2Ge_2$. The solid line indicates an RHF free atom calculation for Mn 3d.

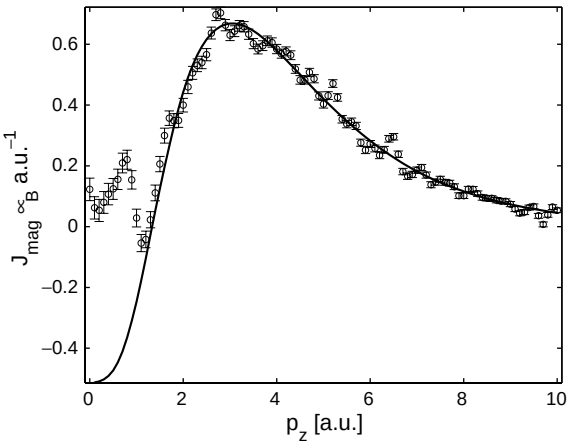


Fig. 2. The experimental magnetic Compton profile (MCP) (circle) of $GdMn_2Ge_2$. The solid line indicates the result of a fit comprising of a combination of RHF free atom calculations for Mn 3d and Gd 4f.

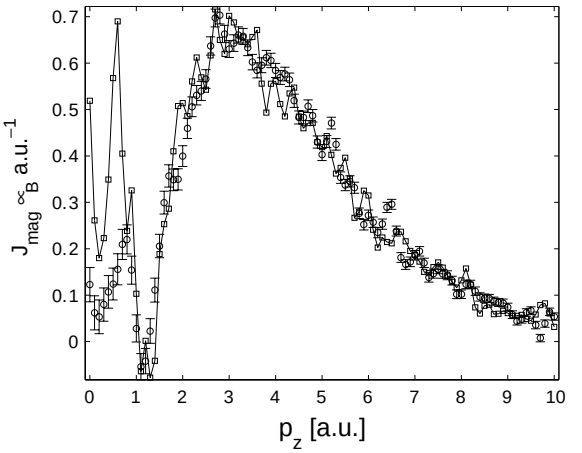


Fig. 3. The experimental magnetic Compton profile (MCP) (circle) and $GdMn_2Ge_2$. The solid line indicates the result of a fit comprising a 4f Gd RHF profile and experimentally measured $LaMn_2Ge_2$.

and vice versa, since the real and momentum space wave functions are related via a Fourier transform: hence, the localized 4f component to the measured EMD is seen as a broad feature in the profile. In order to separate the 4f and 3d moments, the data have been analyzed by fitting a combination of 3d Mn and 4f Gd RHF free atom profiles; in this way, one may easily ascertain the size of the rare-earth site moment. However, to calculate the Mn site moment one must be more careful as the RHF calculation for 3d Mn does not sufficiently account for the solid-state effects and the polarization of the s–p-like conduction band electrons. However, a better approximation to the Mn spin moment in this material is provided by the measured MCP for $LaMn_2Ge_2$, whose spin moment is entirely due to the Mn sites in the structure. Therefore, if one takes a combination of RHF 4f Gd and the experimental profile for $LaMn_2Ge_2$, the overall fit is improved (Fig. 3) and one may comment on the magnitude of the Mn site moment.

From the data analysis, the measured site moment for Gd was determined as $6.8 \pm 0.1\mu_B$ FU$^{-1}$, the Mn moment was determined as $-3.7 \pm 0.1\mu_B$ FU$^{-1}$ oriented antiparallel to the Gd moment. This equates to a site moment of $1.85\mu_B$ per Mn site, again in good agreement with that calculated from magnetization measurements. The difference between the Mn site moments in the La and the Gd compound may be taken to imply that the Mn sublattice is a non-collinear, ferromagnetic structure, with both samples exhibiting different canting angles, resulting from the effect of substituting a large 4f spin moment in place of the non-magnetic La site. The fact that the measured 4f spin moment is closer to the $7\mu_B$ expected for a half-filled 4f shell indicates that the Gd sublattice is ferromagnetically ordered, in $GdMn_2Ge_2$.

From Fig. 3 it is clear that a discrepancy is observed between the fitted and experimental data at low $p_z$, this is attributed to the difference in conduction band electron polarization, which is observed at low $p_z$, caused by the large spin moment on the RE site. The extra conduction band spin polarization extends to $\approx 1.5$ a.u. and is estimated as $0.4 \pm 0.1\mu_B$ FU$^{-1}$.

## 5. Summary

Our results demonstrate that the low temperature spin moments in $LaMn_2Ge_2$ and $GdMn_2Ge_2$ are commensurate with those calculated using a molecular field approximation. Furthermore, they agree with the models proposed suggesting that the

2d Mn sublattice in these materials is a non-collinear arrangement of spins, which is stabilized by a collinear sublattice coming from the rare-earth moment in the Gd compound.

## Acknowledgements

The authors wish to thank the EPSRC(UK) for funding this work, the ESRF for provision of beam time, and V. Honkimaki and T. Buslaps of the high-energy beamline ID15 for their help.

## References

[1] G. Guanghua, et al., J. Magn. Magn. Mater. 214 (2000) 301.
[2] I. Nowik, Y. Levi, I. Felner, E.R. Bauminger, J. Magn. Magn. Mater. 147 (1995) 373.
[3] T. Fujiwara, H. Fujii, Physica B 300 (2001) 198.
[4] H. Fujii, et al., Solid State Commun. 53 (1985) 715.
[5] G.J. Tomka, et al., Phys. Rev. B 58 (1998) 6330.
[6] E.V. Sampathkumaran, et al., Phys. Rev. B 54 (1996) 3710.
[7] Y. Yafet, C. Kittel, Phys. Rev. 87 (1952) 290.
[8] P.M. Platzman, N. Tzoar, Phys. Rev. 2 (1970) 3556.
[9] P. Holm, Phys. Rev. A 37 (1988) 3706.
[10] F. Bell, J. Felsteiner, Phys. Rev. A 53 (1996) R1213.
[11] J.A. Duffy, et al., Phys. Rev. B 61 (2000) 14331.
[12] J.E. McCarthy, et al., Phys. Rev. B 62 (2000) R6073.
[13] J.A. Duffy, et al., J. Phys.: Condens. Matter 10 (1998) 10391.
[14] P. Carra, et al., Phys. Rev. B 53 (1996) R5994.
[15] J.E. McCarthy, et al., J. Synchrotron Radiat. 4 (1997) 102.
[16] J. Felsteiner, P. Pattison, M.J. Cooper, Philos. Mag. 30 (1974) 537.
[17] T. Fujiwara, et al., Phyica B 281 (2000) 161.